



# Simulation of liquid level, temperature and pressure inside a 2000 liter liquid hydrogen tank during truck transportation

Takeda, Minoru ; Nara, Hiroyuki ; Maekawa, Kazuma ; Fujikawa, Shizuichi ; Matsuno, Yu ; Kuroda, Tsuneo ; Kumakura, Hiroaki

---

(Citation)

Physics Procedia, 67:208-214

(Issue Date)

2015

(Resource Type)

journal article

(Version)

Version of Record

(Rights)

©2015. The Authors.

This is an open access article under the CC BY-NC-ND license (<http://creativecommons.org/licenses/by-nc-nd/4.0/>).

(URL)

<https://hdl.handle.net/20.500.14094/90003703>



25th International Cryogenic Engineering Conference and the International Cryogenic Materials Conference in 2014, ICEC 25–ICMC 2014

## Simulation of liquid level, temperature and pressure inside a 2000 liter liquid hydrogen tank during truck transportation

Minoru Takeda<sup>a,\*</sup>, Hiroyuki Nara<sup>a</sup>, Kazuma Maekawa<sup>a</sup>, Shizuichi Fujikawa<sup>b</sup>,  
Yu Matsuno<sup>b</sup>, Tsuneo Kuroda<sup>c</sup>, Hiroaki Kumakura<sup>c</sup>

<sup>a</sup> Graduate School of Maritime Sciences, Kobe University, Kobe, Hyogo 658-0022, Japan

<sup>b</sup> Iwatani Corporation, R&D Center, Aamagasaki, Hyogo 661-0965, Japan

<sup>c</sup> National Institute for Materials Science, Tsukuba, Ibaraki 305-0047, Japan

---

### Abstract

Hydrogen is an ultimate energy source because only water is produced after the chemical reaction of hydrogen and oxygen. In the near future, a large amount of hydrogen, produced using sustainable/renewable energy, is expected to be consumed. Since liquid hydrogen (LH<sub>2</sub>) has the advantage of high storage efficiency, it is expected to be the ultimate medium for the worldwide storage and transportation of large amounts of hydrogen. To make a simulation model of the sloshing of LH<sub>2</sub> inside a 2000 liter tank, simulation analyses of LH<sub>2</sub> surface oscillation, temperature and pressure inside the tank during a truck transportation have been carried out using a multipurpose software ANSYS CFX. Numerical results are discussed in comparison with experimental results.

© 2015 The Authors. Published by Elsevier B.V. This is an open access article under the CC BY-NC-ND license

(<http://creativecommons.org/licenses/by-nc-nd/4.0/>).

Peer-review under responsibility of the organizing committee of ICEC 25-ICMC 2014

**Keywords:** simulation; liquid hydrogen; sloshing; truck transportation

---

---

\* Corresponding author. Tel.: +81-78-431-6329; fax: +81-78-431-6329

E-mail address: [takeda@maritime.kobe-u.ac.jp](mailto:takeda@maritime.kobe-u.ac.jp)

## 1. Introduction

Sustainable and renewable energy such as solar energy, wind energy and tidal energy is very attractive to produce hydrogen, which is expected to be the ultimate energy medium for worldwide storage and transportation. In the storage and transportation of a large amount of hydrogen, liquid hydrogen (LH<sub>2</sub>) has the advantage of high storage efficiency owing to the extremely high density in comparison with gaseous hydrogen (GH<sub>2</sub>). To establish its worldwide storage and land/marine transportation, it is important to develop LH<sub>2</sub> tanks/carriers similar to liquefied natural gas (LNG) tanks/carriers and to elucidate the sloshing conditions inside the tanks during land/marine transportation.

We have studied damped oscillations of a LH<sub>2</sub> surface inside a small vessel under horizontal vibration [1] and the characteristics of a superconducting magnesium diboride level sensor for LH<sub>2</sub> tank [2,3]. Recently, synchronous measurements of LH<sub>2</sub> level, temperature and pressure inside a 2000 liter LH<sub>2</sub> tank have been carried out during truck transportation [4]. A large amount of sloshing of LH<sub>2</sub> with a level exceeding 1200 mm was observed frequently during transportation.

The purpose of the present work is to make a simulation model of sloshing of LH<sub>2</sub> inside a 2000 liter tank during truck transportation using multipurpose software ANSYS CFX.

### Nomenclature

$a, b$	constant every critical point
$a_{a1} \sim a_{a5}$	constant every gas
$C_{a,p}^0$	specific heat at constant zero pressure of $\alpha$ phase
$e_a$	internal energy of $\alpha$ phase
$e_{a,s}$	internal energy of $\alpha$ phase due to phase transition
$e_{\beta,s}$	internal energy of $\beta$ phase due to phase transition
$F_a$	buoyancy of $\alpha$ phase
$f_a$	force vector to $\alpha$ phase
$g$	gravity
$k_a, k_\beta$	heat transfer coefficient of $\alpha$ and $\beta$ phase
$L$	heat of vaporization
$m_{a,\beta}$	mass flow rate from $\beta$ to $\alpha$ phase
$N_p$	number of phase
$P_a$	partial pressure of $\alpha$ phase
$Q_a$	heat to $\alpha$ phase through interface
$R, R_a$	gas constant, gas constant divided by molecular weight
$r_a$	volume fraction of $\alpha$ phase
$S_{Ea}$	heat to $\alpha$ phase from external heat source
$U_a$	velocity vector of $\alpha$ phase
$V, V_a$	volume of small mesh, volume of $\alpha$ phase
$v_a$	specific volume of $\alpha$ phase
$\alpha, \beta$	gaseous phase/liquid phase
$\Gamma_{a\beta}^+$	mass flux from $\beta$ to $\alpha$ phase
$\Gamma_{\beta a}^+$	mass flux from $\alpha$ to $\beta$ phase
$\lambda_a$	thermal conductivity of $\alpha$ phase
$\mu_a$	viscosity of $\alpha$ phase
$\rho_a, \rho_{ref}$	density of $\alpha$ phase, density of reference
$\tau_a$	stress tensor of $\alpha$ phase

## 2. Governing equations

The governing equations employed in ANSYS CFX are as follows:

$$\frac{\partial}{\partial t}(r_\alpha \rho_\alpha) + \nabla \cdot (r_\alpha \rho_\alpha \vec{U}_\alpha) = 0, \quad (1)$$

$$r_\alpha \rho_\alpha \left[ \frac{\partial \vec{U}_\alpha}{\partial t} + (\vec{U}_\alpha \cdot \text{grad}) \vec{U}_\alpha \right] = -\text{grad}(r_\alpha p_\alpha) + r_\alpha \mu_\alpha \Delta \vec{U}_\alpha + \vec{f}_\alpha, \quad (2)$$

$$F_\alpha = (\rho_\alpha - \rho_{ref})g, \quad (3)$$

$$r_\alpha = \frac{V_\alpha}{V}, \quad (4)$$

$$p_\alpha = \frac{RT_\alpha}{v_\alpha - b} - \frac{a(T_\alpha)}{v_\alpha(v_\alpha + b)}, \quad (5)$$

$$C_{\alpha,p}^0 = R_\alpha (a_{\alpha,1} + a_{\alpha,2}T_\alpha + a_{\alpha,3}T_\alpha^2 + a_{\alpha,4}T_\alpha^3 + a_{\alpha,5}T_\alpha^4), \quad (6)$$

$$\begin{aligned} & \frac{\partial}{\partial t}(r_\alpha \rho_\alpha e_\alpha) + \nabla \cdot (r_\alpha \rho_\alpha \vec{U}_\alpha e_\alpha) \\ &= \nabla \cdot (r_\alpha \lambda_\alpha \text{grad} T_\alpha) + r_\alpha \tau_\alpha (\nabla \vec{U}_\alpha)^2 + S_{E_\alpha} + Q_\alpha + \sum_{\beta=1}^{N_p} (\Gamma_{\alpha\beta}^+ e_{\beta S} - \Gamma_{\beta\alpha}^+ e_{\alpha S}) \end{aligned} \quad (7)$$

$$\dot{m}_{\alpha\beta} = \frac{k_\alpha (T_\alpha - T_s) - k_\beta (T_s - T_\beta)}{L}. \quad (8)$$

Here, Eq. (1) is the equation of continuity, Eq. (2) is the equation of motion, Eq. (3) is buoyancy, Eq. (4) describes volume fraction, Eq. (5) is the equation of state, Eq. (6) is the describing specific heat, Eq. (7) is the equation of heat energy and Eq. (8) is the equation of phase generation density.

## 3. Analytical model of the 2000 liter tank

Fig. 1 shows an analytical model and mesh configuration of a 2000 liter tank. As shown in Fig. 1(a), this tank consists of a sideways cylinder with a diameter of 1300 mm, a length of 2083 mm and a volume of 2764 liter in design. In the simulation analysis, the initial volume of LH<sub>2</sub> inside the tank was 1189 liter, which means a LH<sub>2</sub> level of 600 mm. This is the same level as the truck transportation test [4].

As shown in Fig. 1(b), the analytical model of a 2000 liter tank was divided into tetrahedral meshes; the number of meshes was  $1.66 \times 10^6$  and the maximum size of meshes was 16.5 mm.

## 4. Thermal analysis

Temperature profiles of the gaseous phase inside a 2000 liter tank under the static condition were obtained in the following way. First, it was assumed that evaporation and convection of saturated LH<sub>2</sub> (20.3 K) was negligible.

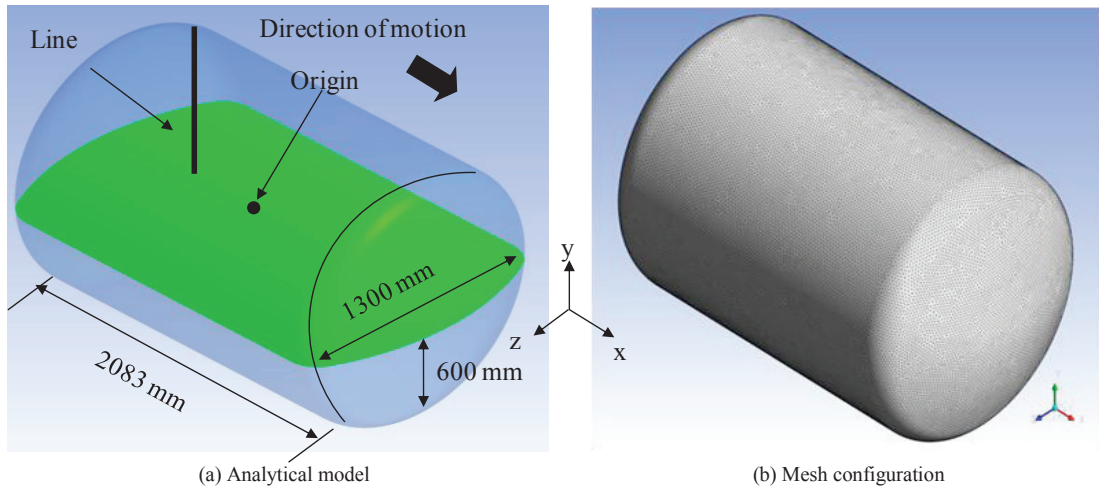


Fig. 1. Analytical model and mesh configuration of the 2000 L tank.

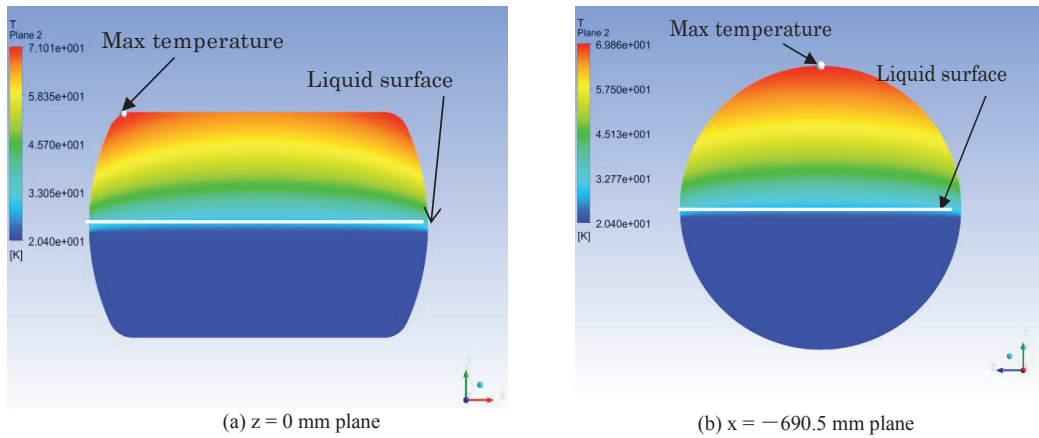


Fig. 2. Temperature distribution in the tank.

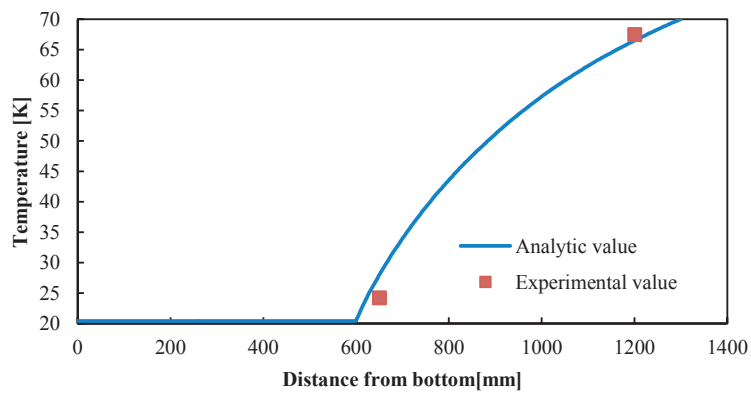


Fig. 3. Temperature distribution along the line in Fig. 1(a).

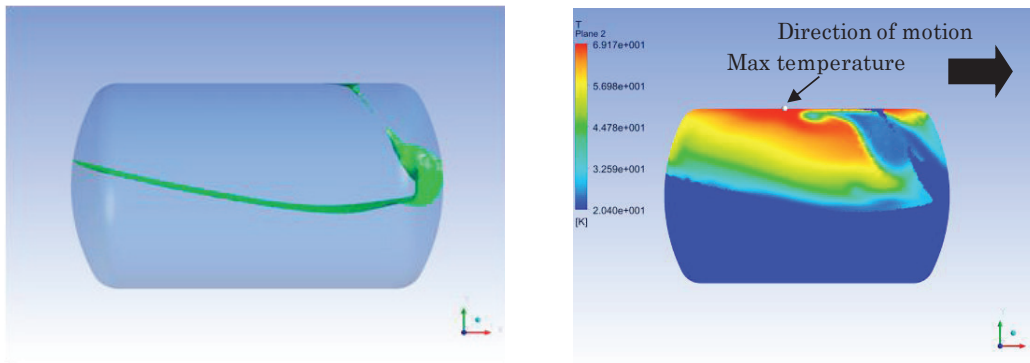
Next, the temperature of  $\text{GH}_2$  was set 20.3 K as an initial condition. Also, the uniform heat leak from the wall of the tank was set at 17 W, which was obtained through the experiment on an increasing rate of the pressure inside the tank under the static condition.

Fig. 2 indicates the temperature distribution in the tank at (a)  $z = 0$  mm plane and (b)  $x = -690.5$  mm plane, where the origin of the coordinates axes ( $x = y = z = 0$ ) was defined as the center of the gravity shown in Fig. 1(a). The maximum temperatures near the top of the tank were 71.0 K and 69.8 K in both Fig. 2 (a) and Fig. 2(b).

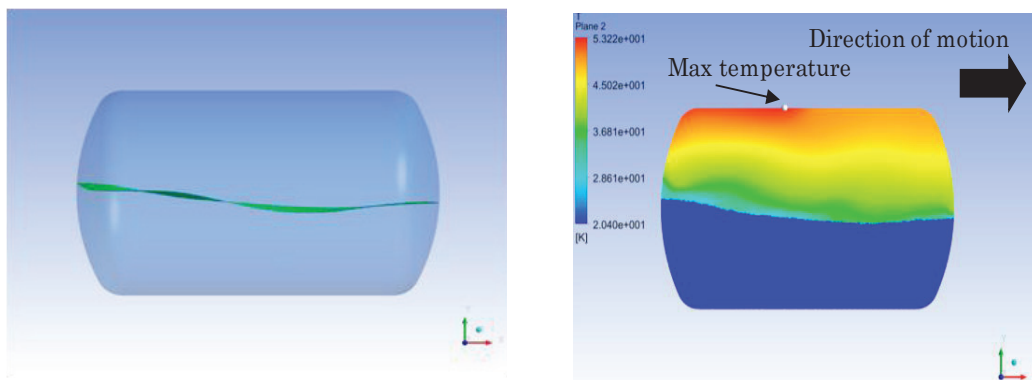
Fig. 3 shows the temperature distribution as a function of the distance from the bottom along the line shown in Fig. 1(a), where  $x = -690.5$  mm and  $z = 0$  mm, comparing the experimental data. It follows that, the numerical results were in good agreement with the experimental results.

## 5. Oscillation and thermal analyses

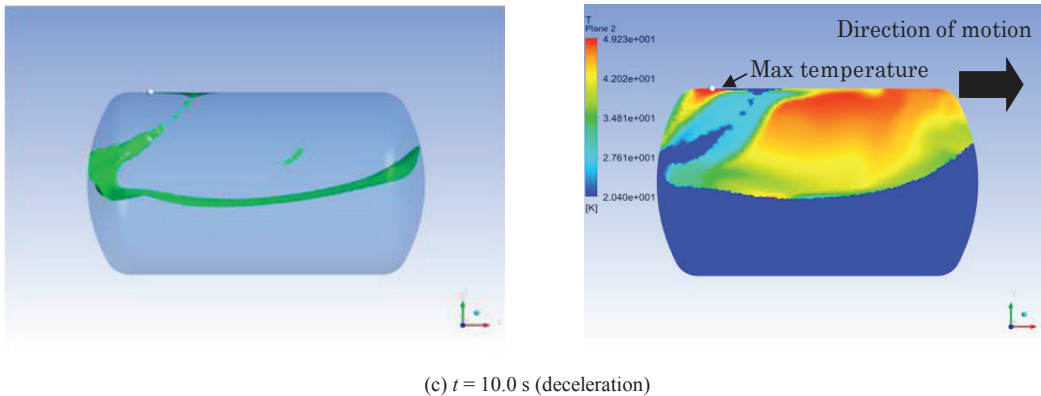
On the basis of the numerical results of thermal analysis, variations in the  $\text{LH}_2$  level, temperature and pressure inside the tank under simple horizontal vibration as a function of time were obtained as following way. First, it was assumed that evaporation of saturated  $\text{LH}_2$  and the heat leak of 17 W were generated. Next, the tank was set to be received acceleration of 0.3 G for 4 s in the direction of an arrow shown in Fig. 1(a), zero acceleration for 4 s with 40 km/h and deceleration of -0.3 G for 4 s. Also, the time step and the total time for simulation analyses were 0.01 s and 12 s, respectively.



(a)  $t = 2.0$  s (acceleration)



(b)  $t = 8.0$  s (uniform velocity)



(c)  $t = 10.0$  s (deceleration)  
 Fig. 4. Position of liquid surface (left) and temperature distribution in the plane of  $z = 0$  mm (right).

Fig. 4 shows the position of liquid surface and the temperature distribution in the plane of  $z = 0$  mm at (a)  $t = 2.0$  s (acceleration), (b)  $t = 8.0$  s (uniform velocity) and (c)  $t = 10.0$  s (deceleration). The maximum temperatures nearly the top of the tank were 66.5 K at  $t = 2.0$  s, 52.3 K at  $t = 8.0$  s and 49.2 K at  $t = 10.0$  s. As shown in Fig. 4, wide-ranging cooling of the gaseous phase is believed to be caused by sloshing of  $\text{LH}_2$ .

Figure 5 indicates time chart of the  $\text{LH}_2$  level and the temperature of  $\text{GH}_2$  along the line in Fig. 1(a), where the data point of temperature was set at 1200 mm from the bottom of the tank. Also, time chart of the average pressure based on atmospheric pressure and the average temperature of  $\text{GH}_2$  in the tank are shown in Fig. 6. As is seen in Fig. 5, the period of oscillation of  $\text{LH}_2$  level was 2 s and the maximum level was 1054 mm. These results were similar to those of the truck transportation test. Average pressure decreased from 0.032 MPa/gauge to 0.014 MPa/gauge with decreasing average temperature of  $\text{GH}_2$  from 47.8 K to 39.1 K in Fig. 6, showing qualitative agreement with results of the truck transportation test. It appears that  $\text{LH}_2$  surface oscillation, temperature and pressure inside the tank during transportation can be demonstrated by an ANSYS CFX.

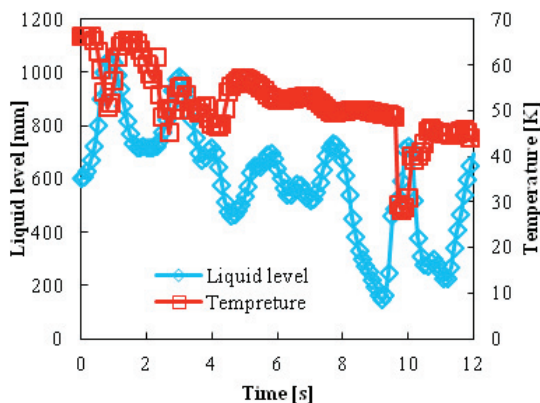


Fig. 5. Time chart of liquid level and temperature of  $\text{GH}_2$  in 2000 L tank.

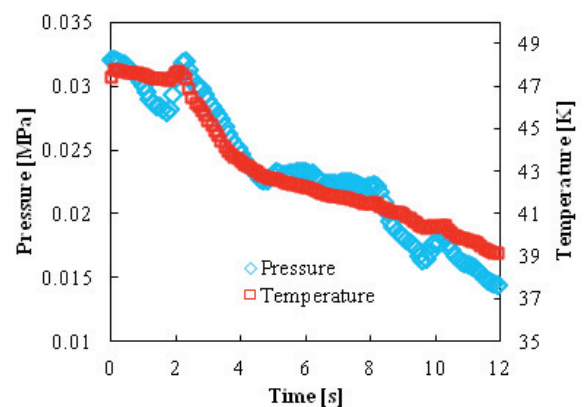


Fig. 6. Time chart of average pressure and average temperature of  $\text{GH}_2$  in 2000 L tank.

## 6. Summary

Simulation of  $\text{LH}_2$  surface oscillation, temperature and pressure inside a 2000 liter tank during truck transportation were carried out using an ANSYS CFX. Periodic oscillation of  $\text{LH}_2$  level, maximum  $\text{LH}_2$  level over 1000 mm and decreasing average pressure with decreasing average temperature inside the tank, which were observed in the truck transportation test, were demonstrated successfully. Oscillation and thermal analyses of a large  $\text{LH}_2$  tank of  $1250 \text{ m}^3$  for marine transportation will be carried out as a future work.

## Acknowledgements

This work was supported in part by a Grant-in Aid for Scientific Research, JSPS KAKENHI Grant Number 24246143, Japan.

## References

- [1] M. Takeda, S. Yagi, I. Kodama, S. Fujikawa, H. Kumakura, and T. Kuroda: Liquid Hydrogen Experiment Facility with System Enabling Observation under Horizontal Vibration, *Adv. Cryo. Eng.*, Vol.55 (2010) pp. 311-318.
- [2] M. Takeda, Y. Matsuno, I. Kodama, H. Kumakura and C. Kazama: Application of MgB<sub>2</sub> Wire to Liquid Hydrogen Level Sensor — External-Heating-Type MgB<sub>2</sub> Level Sensor, *IEEE Trans. Appl. Supercond.* Vol.19 (2009) pp.764-767.
- [3] K. Maekawa, M. Takeda, Y. Matsuno, S. Fujikawa, T. Kuroda and H. Kumakura: Thermal response of MgB<sub>2</sub> level sensor for liquid hydrogen using external heater, *Proceeding of ICEC24-ICMC2012* (2013) pp. 59-62.
- [4] M. Takeda, S. Fujikawa, Y. Matsuno, K. Maekawa, T. Kuroda and H. Kumakura: Synchronous measurements of liquid level, temperature and pressure inside a 2000 liter liquid hydrogen tank during a track transportations, *Proceedings of ICEC24-ICMC2012* (2013) pp. 311-314.